

Trivacancy and trivacancy-oxygen complexes in silicon: Experiments and *ab initio* modelingV. P. Markevich,¹ A. R. Peaker,¹ S. B. Lastovskii,² L. I. Murin,² J. Coutinho,³ V. J. B. Torres,³ P. R. Briddon,⁴ L. Dobaczewski,⁵ E. V. Monakhov,⁶ and B. G. Svensson⁶¹*School of Electrical and Electronic Engineering, University of Manchester, Manchester M60 1QD, United Kingdom*²*Scientific-Practical Materials Research Centre, NAS of Belarus, P. Brovka Str. 19, Minsk 220072, Belarus*³*I3N, University of Aveiro, Campus Santiago, 3810-193 Aveiro, Portugal*⁴*School of Natural Science, University of Newcastle upon Tyne, Newcastle-upon-Tyne NE1 7RU, United Kingdom*⁵*Institute of Physics, Polish Academy of Sciences, Al. Lotnikow 32/46, 02-668 Warsaw, Poland*⁶*Department of Physics, Oslo University, N-0316 Oslo, Norway*

(Received 25 September 2009; revised manuscript received 27 November 2009; published 30 December 2009)

A center from the family of “fourfold coordinated (FFC) defects”, previously predicted theoretically, has been experimentally identified in crystalline silicon. It is shown that the trivacancy (V_3) in Si is a bistable center in the neutral charge state, with a FFC configuration lower in energy than the (110) planar one. V_3 in the planar configuration gives rise to two acceptor levels at 0.36 and 0.46 eV below the conduction band edge (E_c) in the gap, while in the FFC configuration it has trigonal symmetry and an acceptor level at $E_c - 0.075$ eV. From annealing experiments in oxygen-rich samples, we also conclude that O atoms are efficient traps for mobile V_3 centers. Their interaction results in the formation of V_3O complexes with the first and second acceptor levels at $E_c - 0.46$ eV and $E_c - 0.34$ eV. The overall picture, including structural details, relative stability, and electrical levels, is accompanied and supported by *ab initio* modeling studies.

DOI: [10.1103/PhysRevB.80.235207](https://doi.org/10.1103/PhysRevB.80.235207)

PACS number(s): 61.72.jd, 61.72.Bb, 61.80.Fe, 71.55.Cn

I. INTRODUCTION

A new type of topological defects in semiconductor crystals, the so-called “fourfold coordinated (FFC) defects,” has been predicted by *ab initio* modeling studies,^{1–3} but so far there has been no solid experimental evidence for their existence. We present experimental and *ab initio* modeling results, which show that the trivacancy (V_3) in silicon is a bistable center in the neutral charge state, where a fourfold coordinated configuration is the energetically favorable one. An acceptor level is assigned to the FFC V_3 defect and its atomic symmetry is determined by means of high-resolution Laplace deep-level transient spectroscopy (LDLTS) combined with uniaxial stress.

Vacancy-related clusters (V_n) in silicon are technologically important defects because of their role in capturing unwanted impurities and silicon interstitials so reducing enhanced diffusion of dopants in extremely scaled integrated circuits. Such clusters have attracted a great attention recently.^{3–6} Among the small V_n ($n \leq 5$) defects, only the divacancy (V_2) has been studied extensively experimentally and theoretically^{4,7–11} and its properties are reasonably well understood. The available information on the properties of V_3 , V_4 , and V_5 defects is limited and controversial,^{3–5,12} but in general it is thought that the minimum-energy structures for the neutral V_n defects with n from 3 to 5 could have “part of a hexagonal ring” (PHR) configurations.^{4,5} However, from electron-spin-resonance (ESR) studies of neutron-irradiated Si, only the V_3 defect structure is consistent with the PHR configuration (the Si-A4 ESR signal was assigned to V_3).¹² The A3 and P3 ESR signals were attributed to different configurations of V_4 and P1 ESR signal was assigned to V_5 ,¹² but neither of the suggested defect structures associated with these signals coincides with the PHR configurations of tetra- and pentavacancy.^{4,5} Furthermore, it has been ar-

gued recently that the fourfold coordinated configurations are lower in energy for the V_3 to V_5 defects than the PHR ones.³ No clear experimental evidence of the existence of V_n clusters in the fourfold coordinated configurations have been presented so far and electronic properties of the defects in both configurations are not well understood.

It is shown in the present work that V_3 is bistable in the neutral charge state, with the fourfold coordinated configuration being lower in energy than the (110) planar configuration. V_3 in the (110) planar configuration gives rise to two acceptor levels at 0.36 and 0.46 eV below the conduction band edge (E_c), while in the fourfold coordinated configuration, the defect has trigonal symmetry showing an acceptor level at $E_c - 0.075$ eV. V_3 is mobile in Si at temperatures higher than 200 °C and can be trapped by an oxygen atom so resulting in the appearance of a V_3O defect. The V_3O center is only stable in the (110) planar configuration and gives rise to two acceptor levels at $E_c - 0.34$ eV and $E_c - 0.455$ eV. Some preliminary results on the study of the V_3 center have been published by us in Ref. 13.

II. EXPERIMENTAL AND MODELING DETAILS

Experimental results in the present work were obtained by means of deep-level transient spectroscopy (DLTS) and high-resolution Laplace DLTS in combination with uniaxial stress.¹⁴ Samples for the study were prepared from phosphorus-doped epi-Si ($\rho \approx 30 \Omega \text{ cm}$), which was grown on highly Sb-doped ($\rho \approx 0.01 \Omega \text{ cm}$) bulk Czochralski-grown Si (Cz-Si) wafers. P^+-n diodes were formed by implantation of boron ions with subsequent annealing at 1200 °C in nitrogen ambient. Oxygen concentration in the epilayers was determined from the rate of transformation of the divacancy to the divacancy-oxygen (V_2O) defect with the use of data presented in Ref. 9. The oxygen concentration

was close to $4 \times 10^{17} \text{ cm}^{-3}$ in all the epi-Si samples. Also a few samples from a phosphorus-doped ($\rho \approx 80 \text{ } \Omega \text{ cm}$) Si ingot, which was refined by float-zone (FZ) technique in vacuum, were studied. According to results of infrared-absorption measurements, the oxygen concentration in the FZ-grown samples was lower than $5 \times 10^{15} \text{ cm}^{-3}$. For uniaxial stress measurements, we used three $1 \times 2 \times 7 \text{ mm}^3$ bars with each of the long axes oriented in one of the three main crystallographic directions. The samples for uniaxial stress measurements were cut from a Czochralski-grown Si crystal, which was doped with phosphorus to $3 \times 10^{14} \text{ cm}^{-3}$ and had oxygen and carbon concentrations about $8 \times 10^{17} \text{ cm}^{-3}$ and $2 \times 10^{16} \text{ cm}^{-3}$, respectively. Schottky barrier diodes were prepared on the FZ-grown samples and oriented bars by thermal evaporation of Au through a shadow mask. All the samples were irradiated with 6 MeV electrons using a linear accelerator. The flux of electrons was $1 \times 10^{12} \text{ cm}^{-2} \text{ s}^{-1}$ and the temperature of the samples during irradiation did not exceed $50 \text{ }^\circ\text{C}$. Thermal anneals of the irradiated structures were carried out in a furnace in a dry N_2 ambient.

Ab initio calculations were carried out with a pseudopotential density-functional code, (AIMPRO),¹⁵ along with the local-density approximation for the exchange-correlation potential.¹⁶ Basis sets for valence states are atom-centered *s*- and *p*-like Gaussian functions with four optimized exponents together with *d*-polarization functions (further details and convergence tests may be found elsewhere¹⁷). In order to avoid dispersive gap states as well as to account for the considerable strain fields that may occur around vacancy complexes in Si,¹⁸ the crystalline host was modeled as H-terminated spherical clusters with up to 424 Si atoms. All atomic sites except the outer Si-H units were allowed to relax with help of a conjugate gradient algorithm. Enthalpies for electron emission (acceptor levels) are calculated by comparing the electron affinity of the defect (A_d) to that of a marker defect (A_m) which has well-established level location in the gap $E_c - E_{m,\text{exp}}$. This procedure has been employed with success on defects in Si and Ge.^{17,19} Accordingly, $E_{\text{cal}}(q - 1/q) = E_{m,\text{exp}}(q - 1/q) + A_m(q - 1/q) - A_d(q - 1/q)$, with $A(q - 1/q) = E(q - 1) - E(q)$, where $E(q)$ is the total energy of a defect cluster with net charge q . For the marker, we choose the V_2O complex with first and second acceptor levels measured at $E_c - 0.47 \text{ eV}$ and $E_c - 0.23 \text{ eV}$, respectively.^{9,10}

III. EXPERIMENTAL RESULTS AND THEIR DISCUSSION

Figure 1(a) shows DLTS spectra for an epi-Si p^+-n diode which was irradiated with 6 MeV electrons and then subjected to 30 min heat treatments at $125 \text{ }^\circ\text{C}$ and $300 \text{ }^\circ\text{C}$. All peaks in the spectra except the one with its maximum at about 63 K are related to radiation-induced defects. Electronic signatures [activation energy for electron emission (E_n) and pre-exponential factor (α) or apparent capture cross section (σ_{na})] were determined from Arrhenius plots of electron emission rates for all the traps. A comparison of the values for traps responsible for the peaks having their maxima at 63, 91, and 130 K in the spectra 1 and 2 with

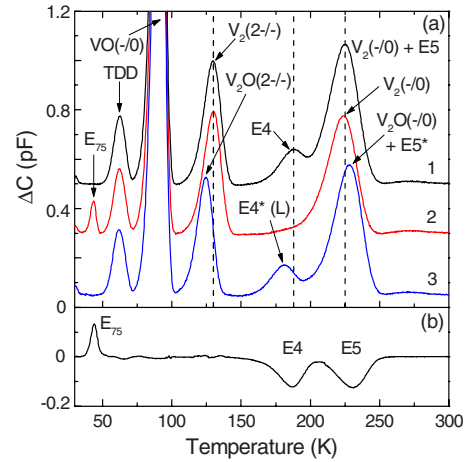


FIG. 1. (Color online) (a) DLTS spectra for an epi-Si p^+-n diode which was subjected to the following subsequent treatments: (1) irradiation with 6 MeV electrons to a dose of $8 \times 10^{13} \text{ cm}^{-2}$; (2) and (3) 30 min anneals at $125 \text{ }^\circ\text{C}$ and $300 \text{ }^\circ\text{C}$, respectively. Measurement settings were $e_n = 80 \text{ s}^{-1}$, bias $-10 \text{ V} \rightarrow -2 \text{ V}$, and pulse length 1 ms. The spectra are shifted on the vertical axis for clarity. (b) Difference between the DLTS spectra 2 and 1 in (a).

those known from the literature allows us to associate these peaks with electron emissions from the positive charge state of thermal double donors,²⁰ the negative charge state of the vacancy-oxygen (VO) complex,^{10,21} and the double negative charge state of V_2 ,⁸⁻¹⁰ respectively.

It was found that the capacitance transients measured with the use of Laplace DLTS (Fig. 2) in the temperature range $210\text{--}240 \text{ K}$ for the as-irradiated diode (spectrum 1 in Fig. 1) consist of contributions of emissions from two electron traps. Electronic signatures of the trap responsible for the signal with the higher magnitude in the spectrum of the as-irradiated sample in Fig. 2 are consistent with those for electron emission from the singly negatively charged state of the divacancy.⁸⁻¹⁰ The magnitude of the signal with the lower magnitude in this spectrum is equal to that of the trap responsible for the peak with its maximum at about 187 K in Fig. 1.

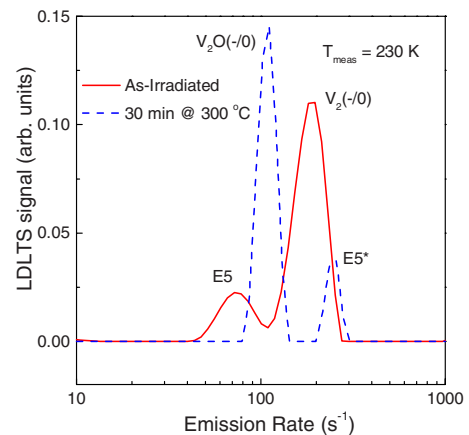


FIG. 2. (Color online) Laplace DLTS spectra measured at 230 K for an epi-Si p^+-n diode, which was irradiated with 6 MeV electrons to a dose of $8 \times 10^{13} \text{ cm}^{-2}$ and subsequently annealed at $300 \text{ }^\circ\text{C}$ for 30 min.

TABLE I. Electronic parameters of V_3 -related acceptor levels in Si obtained from LDLS measurements and positions of the energy levels derived from *ab initio* calculations. Values of the apparent capture cross section (σ_{na}) were calculated by dividing the α values by a constant of $6.54 \times 10^{21} \text{ s}^{-1} \text{ K}^{-2} \text{ cm}^{-2}$.

Defect label	Assignment	E_{na} (eV)	α ($\text{s}^{-1} \text{ K}^{-2}$)	σ_{na} (cm^2)	$E_{cal}(q-1/q)$ (eV)
E4 (E4a)	$V_3(2-/-)$	0.359	1.4×10^7	2.15×10^{-15}	0.28
E5 (E4b)	$V_3(-/0)$	0.458	1.6×10^7	2.4×10^{-15}	0.50
E_{75}	$V_3^*(-/0)$	0.075	2.4×10^7	3.7×10^{-15}	0.12
$E4^*$	$V_3O(2-/-)$	0.337	7.85×10^6	1.2×10^{-15}	0.28
$E5^*$	$V_3O(-/0)$	0.455	4.0×10^7	6.1×10^{-15}	0.42

It appears that the two later electron emission signals can be associated with the E4 and E5 (or E4a and E4b) traps studied in irradiated silicon diodes and transistors in recent papers.^{22–26} So, in the following, we will refer to these emission signals as related to the E4 and E5 traps. Some values of electronic signatures for the E4 and E5 traps have been published,^{22–26} however, those values were mainly determined by conventional DLTS and overlapping of the emission signals caused by the E4 and E5 traps with the much stronger one due to the $V_2(-/0)$ transition limited the accuracy of the deduced values. The application of Laplace DLTS technique allows us to separate readily the electron emission signals due to the E4 and E5 traps from that due to the $V_2(-/0)$ transition (Fig. 2) and to determine the electronic signatures of these traps with high accuracy. The values obtained are listed in Table I.

We have also observed the E4 and E5 traps in float-zone-grown Si samples with low oxygen content after irradiation with 6 MeV electrons. In the irradiated FZ-Si samples, the vacancy-phosphorus pair²⁷ was the dominant vacancy-related radiation-induced defect. The E4 and E5 traps were introduced in FZ-Si samples with similar rates as in epi-Si p^+-n diodes upon electron irradiation. The two traps annealed out at the same rates upon isochronal or isothermal anneals in the temperature range 50–125 °C and in addition they disappeared at the same rates in both the epi-Si p^+-n diodes and FZ-Si samples. Our data on the annealing behavior of the E4 and E5 traps are consistent with those obtained in Refs. 22 and 24, where on the basis of an analysis of the annealing results, a conclusion was drawn that these traps are related to two different energy levels of the same defect. It is found in the present work that simultaneously with the disappearance of these traps another defect, which gives rise to a peak with its maximum at about 44 K, appeared in the DLTS spectra for both types of samples [see, e.g., Fig. 1(b) and spectrum 2 in Fig. 1(a)]. The E_n value of this trap was found to be 0.075 eV (Table I) and it will be referred to as the E_{75} trap. Figure 3 shows changes in the normalized concentrations of the E4 and E_{75} traps in a p^+-n diode upon isothermal annealing at 77 °C. An analysis shows that both the decay of the E4 trap and the growth of the E_{75} trap can be described by monoexponential functions with matching decay and growth rates. In this context, it should be emphasized that the maximum absolute concentrations of the traps are the same and hence, the clear anticorrelation between the normalized values in Fig. 3 holds also on an absolute scale.

Evidently, the formation of the E_{75} trap is directly related to the disappearance of the E4 and E5 traps.

In agreement with results presented in Ref. 26, we have found that an application of forward bias injection with a current density in the range 10–15 A/cm² for 20 min at 300 K to the irradiated p^+-n diodes, which before biasing were annealed in the temperature range 50–200 °C, resulted in the complete regeneration of the E4 and E5 peaks and also in the disappearance of the E_{75} trap. Furthermore, it was found from many experiments with the sequential annealing and injection treatments that the $E4(E5) \leftrightarrow E_{75}$ transformations are fully reversible. It should also be noted that the $E4(E5) \leftrightarrow E_{75}$ transformations in the electron-irradiated samples studied did not result in significant changes in concentrations of the VO and V_2 centers [see, e.g., Fig. 1(b)].

The E4 and E5 signals were associated in Refs. 22–26 with two different energy levels of the same intrinsic defect which appears in Si samples after irradiations with high-energy particles (electrons with $E > 2$ MeV, ions, neutrons, etc.). Our results on the introduction rates of the E4 and E5 traps in different samples by electron irradiation, on the annealing behavior of the traps, and on injection-induced transformations are fully consistent with the above suggestions. Further, it is shown in the present work that the defect can exist in two configurations with different electronic properties. We have carried out LDLS measurements under uniaxial stress for the E_{75} trap in order to obtain more infor-

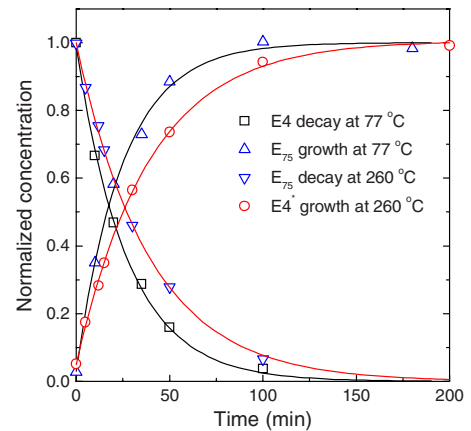


FIG. 3. (Color online) Changes in normalized concentrations (N/N_{max}) of E4, E_{75} , and $E4^*$ traps upon isothermal anneals of an electron-irradiated epi-Si p^+-n diode at 77 °C and 260 °C.

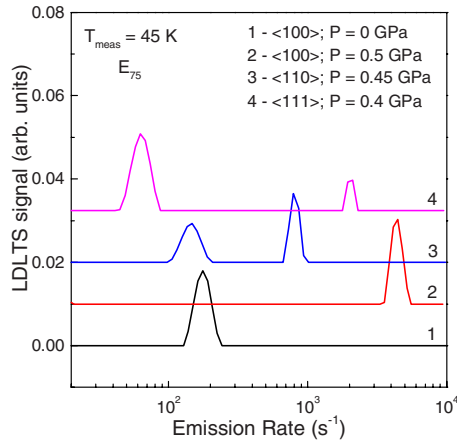


FIG. 4. (Color online) Laplace DLTS spectra of the E_{75} trap taken at 45 K with no stress and the stress applied along three major crystallographic directions of the Cz-Si samples.

mation about the structure of the center in this configuration. Figure 4 shows the LDLS splitting pattern for the E_{75} trap under application of uniaxial stress to three samples with the long axis oriented along each of the three main crystallographic directions. It was found that the observed splitting pattern is characteristic for a center with trigonal symmetry:²⁸ for the stress orientation along the $\langle 100 \rangle$ direction no line splitting is observed, while for stress in the $\langle 110 \rangle$ and $\langle 111 \rangle$ directions, the Laplace DLTS peak splits into two components with the amplitude ratios 1:1 and 3:1, respectively. The magnitudes of the split lines sum to the value for the unstressed sample. We have tried to study a response of the E4 trap to uniaxial stress but this experiment has not been successful because the LDLS line due to the E4 trap is rather close to the much stronger line due to electron emission from the first acceptor level of divacancy and the line due to the E5 trap. Splitting of all three lines under application of stress results in several overlapping emission signals and, consequently, in an unreliable Laplace DLTS analysis.

There were only negligible changes in the DLTS spectra upon isochronal annealing of the irradiated p^+n diodes in the temperature range 125–200 °C. Heat treatments in the temperature range 200–275 °C resulted in the disappearance of both acceptor states of V_2 and the E_{75} trap (or the E4-E5 pair after injection treatments) and the appearance of four other emission signals (Figs. 1, 2, and 5). Electronic signatures of two of them were identical to those for two acceptor states of the V_2O defect.^{9,10} An almost one-to-one correlation was observed between the loss of the E_{75} trap and creation of $E4^*$ and $E5^*$, electronic signatures of which were similar to those of the E4 and E5 traps (Table I). Figure 3 shows the kinetics of the decay of the E_{75} trap and formation of the $E4^*$ trap upon isothermal annealing at 260 °C. Both kinetics are described well by monoexponential functions with the same rates. These were found to be very close to those of the decay of V_2 and formation of the V_2O complexes in p^+n diodes. The transformation of the E_{75} trap into the $E4^*$ - $E5^*$ pair occurred only in p^+n diodes made from epitaxial material containing oxygen and not in FZ-Si samples. In the irradiated FZ-Si samples, the E_{75} trap did not disappear even

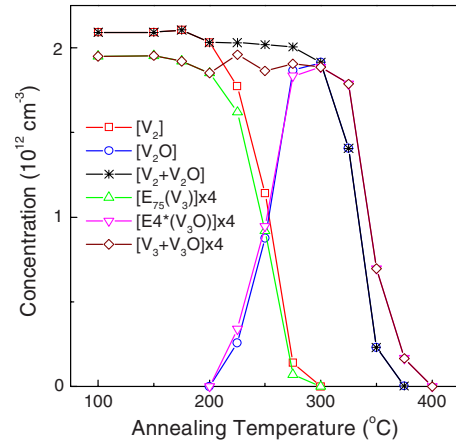


FIG. 5. (Color online) Changes in concentrations of divacancy- and trivacancy-related defects upon 30 min isochronal annealing of an electron-irradiated epi-Si p^+n diode. Concentrations of the V_3 -related defects are multiplied by 4.

after anneals at temperatures as high as 400 °C.

In previous studies, the E4 and E5 traps were assigned to either V_3 or V_4 centers or to the di-interstitial-oxygen (I_2O) complex.^{22,24,25} It was argued in Ref. 26 that the E4-E5 pair could be associated with a primary defect located in defect clusters and closely related to the divacancy. Particularly, the divacancy perturbed by strain associated with the clusters was mentioned.²⁶ Some properties of the defect, which is responsible for the E4-E5 traps in the electron-irradiated samples studied, are indeed similar to those of V_2 . Both centers possess two acceptor levels in the upper part of the band gap and their elimination rates in oxygen-rich Si samples upon anneals in the temperature range 200–275 °C are nearly the same. However, from the LDLS results, we can firmly conclude that our irradiation procedure, unlike ion implantation or neutron irradiation, introduces only point defects uniformly distributed in the probed volumes and not perturbed by any strain. The results obtained in the present work including the results of uniaxial stress measurements can only be explained consistently when the E4 and E5 traps are assigned to V_3 in the (110) planar configuration and the E_{75} trap to V_3 in the “fourfold” configuration. These assignments are consistent with all the results available in the literature on introduction rates, electronic properties, structure, and thermal stability of the V_3 defect and explain the controversies mentioned earlier.^{3,4,12,22,26,29}

There is strong experimental evidence that the elimination of divacancies in oxygen-rich Si samples is associated with their interaction with oxygen atoms and results in the formation of a V_2O defect. The DLTS signatures of V_2O are very similar to those of V_2 .^{9,10} The electronic signatures of the $E4^*$ and $E5^*$ traps are also very similar to those of their E4 and E5 precursors indicating that the former traps could be related to a complex of the original center and an oxygen atom. So, it is reasonable to assign the $E4^*$ and $E5^*$ traps to acceptor states of the V_3O complex. The electronic signatures and formation kinetics of the $E4^*$ trap resemble those for the L center, which was observed in Si diodes irradiated with 15 MeV electrons and annealed at 205–285 °C.³⁰ It was argued

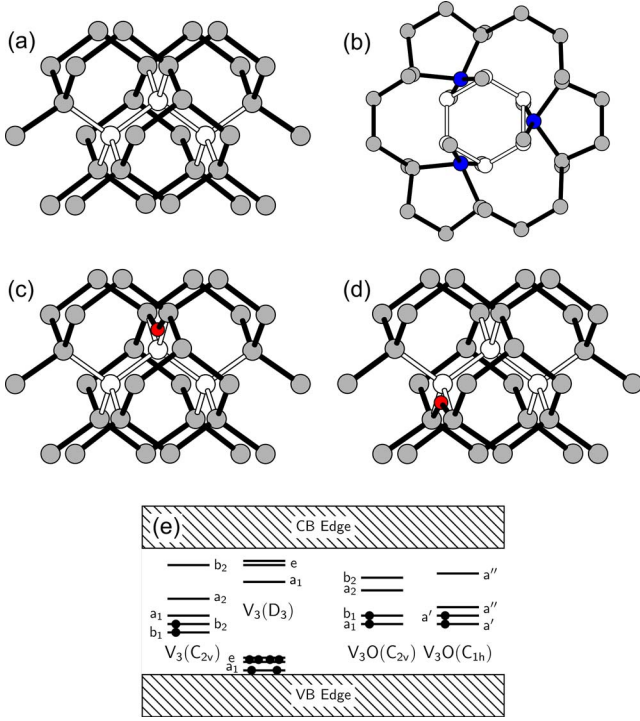


FIG. 6. (Color online) Atomic structures of (a) $V_3(C_{2v})$, (b) $V_3(D_3)$, (c) $V_3O(C_{2v})$, and (d) $V_3O(C_{1h})$. $V_3(D_3)$ is represented along the $\langle 111 \rangle$ direction, whereas other structures are viewed approximately along $\langle 110 \rangle$. Silicon, oxygen, and vacancy sites are represented as gray, red (two-fold coordinated), and white balls, respectively. Three Si interstitial atoms in (b) are represented as dark blue balls. In (e), we depict the one-electron picture for all four defects of interest obtained from the Kohn-Sham states within the valence-band (VB) and conduction-band (CB) edges (band gap of the cluster is $E_g = 2.4$ eV). Spin-up and spin-down occupied states are represented as left- and right-hand circles, respectively.

in Ref. 30 that the L center could be related to the V_3O defect.

It should be noted that our results on the annealing behavior of the traps assigned by us to the V_3 and V_3O defects are fully consistent with the results on the annealing behavior of V_3 obtained in ESR studies²⁹ and on the formation of the V_3O center obtained in a recent infrared-absorption study.³¹ It is also worth mentioning that according to our preliminary DLTS results on the electron-irradiated n^+-p diodes and *ab initio* modeling, both the V_3 and V_3O centers also give rise to two donor levels in the lower part of the gap.

IV. AB INITIO MODELING RESULTS

While multivacancy centers may be regarded as the removal of adjoining Si atoms [see Fig. 6(a)], a rather different approach was proposed in the calculations of Makhov and Lewis³ who showed that three self-interstitials could decorate all 12 dangling bonds in V_6 resulting in a low-energy fourfold coordinated V_3 complex [see Fig. 6(b)]. We have also investigated several structures for V_3 and particular attention was paid to the most stable forms, namely, the PHR V_3 made up of three neighboring vacant sites with C_{2v} sym-

metry, $V_3(C_{2v})$ shown in Fig. 6(a), and the fourfold coordinated form with D_3 symmetry, $V_3(D_3)$ shown in Fig. 6(b). In line with Ref. 3, we found that neutral diamagnetic $V_3(D_3)$ is 0.50 eV more stable than diamagnetic $V_3(C_{2v})$ and also 0.23 eV more stable than paramagnetic spin-1 $V_3(C_{2v})$. After adding and removing electrons to the system, $V_3(D_3)$ turns to be metastable by 1.19, 0.43, 0.05, and 0.50 eV for double plus, plus, minus, and double minus charge states, respectively, where $V_3(C_{2v})$ stands now as the ground state. We have investigated the electronic structure of these complexes by inspection of the one-electron levels shown in Fig. 6(e). It is found that the long and twisted bonds in $V_3(D_3)$ give rise to states close to the band edges as in amorphous silicon, whereas silicon radicals in $V_3(C_{2v})$ lead to much deeper states around midgap. Let us first look in detail at the latter and more ordinary form of the defect shown in Fig. 6(a). $V_3(C_{2v})$ comprises two remote silicon dangling-bond radicals lying on the (110) symmetry plane of Fig. 6(a), plus three long reconstructed Si-Si bonds perpendicular to the same plane. While the end radicals give rise to b_1 and a_1 gap states [Fig. 6(e)], the reconstructions produce three bonding states below the valence-band top and corresponding antibonding states (b_2 , a_2 , and b_2) in the forbidden gap. As we show in Fig. 6(e), the lower b_2 level is responsible for the acceptor activity of the defect. We note that all three Si-Si reconstructions are very similar and their proximity leads to a strong electronic coupling between the isosymmetric b_2 levels. Consequently, these move away from the a_2 state. The electronic structure of $V_3(D_3)$ arises from twelve 2.6–2.7 Å long and twisted Si-Si bonds which hybridize into bonding and antibonding a_1 and e gap levels [Fig. 6(e)]. The upper a_1 state has essentially an antibonding character between interstitial silicon atoms [represented as dark blue balls in Fig. 6(b)] and their neighbors at the core of the defect. It has therefore the right attributes to be responsible for a shallow acceptor trap such as the E_{75} .

Adding one electron to $V_3(C_{2v})$ gives $A(-/0) = -3.48$ eV for its first electron affinity. A similar calculation for V_2O results in $A(-/0) = -3.45$ eV, i.e., 0.03 eV above the value of V_3 . Accordingly, considering that the first acceptor level of V_2O lies at $E_c - 0.47$ eV,^{9,10} we place the first acceptor level of $V_3(C_{2v})$ at $E_c - 0.50$ eV. Proceeding to the second electron affinity, we find that $A(=/-) = -2.16$ eV for $V_3(C_{2v})$, which lies 0.05 eV below the same quantity for V_2O . This places the second acceptor level of $V_3(C_{2v})$ at $E_c - 0.28$ eV. Similar calculations for $V_3(D_3)$ result in first and second emission enthalpies of 0.23 and -0.10 eV. These results indicate that while $V_3(C_{2v})$ possess first and second acceptor levels close to E_5 and E_4 , respectively, $V_3(D_3)$ is only able to trap a single weakly bound electron, i.e., in agreement with the E_{75} trap measurements.

It has been previously reported that the marker method works best when the acceptor (or donor) states from both the scrutinized defect being studied and the marker have a similar character, i.e., symmetry and space extent.¹⁹ The acceptor level of the structure shown in Fig. 6(b) arises from an antibonding state on long Si-Si bonds, making the VO complex with its long Si-Si reconstruction a better marker for this defect. The Si-Si antibonding state in VO produces an acceptor level at $E_c - 0.17$ eV,^{10,21} and comparing electron affini-

ties of $V_3(D_3)$ and VO, we place the acceptor level of $V_3(D_3)$ at $E_c - 0.12$ eV. This further supports our assignment of $V_3(D_3)$ to the E_{75} trap.

The interaction of V_3 with an interstitial oxygen atom was also investigated by calculations. The effect is that the O atom stabilizes the planar structure and the V_3O complex with C_{2v} symmetry shown in Fig. 6(c) is the ground state for neutral, positively, and negatively charged defects. Here, the O atom bridges the Si-Si reconstruction at the center of the defect. Neutral defects were found to be energetically favorable in the spin-1 state for both $V_3O(C_{2v})$ and $V_3O(C_{1h})$. The latter is metastable by 0.36 eV and it is depicted in Fig. 6(d). A fourfold coordinated V_3O complex [after binding an oxygen atom to a $V_3(D_3)$ structure] is metastable by at least 0.2 eV. Using the marker method and comparing electron affinities of $V_3O(C_{2v})$ to those of V_2O , we place $V_3O(-/0)$ and $V_3O(=/-)$ at $E_c - 0.42$ eV and $E_c - 0.28$ eV, respectively. Both levels are less than 0.1 eV away from the analogous levels calculated for $V_3(C_{2v})$ and their respective assignments to $E5^*$ and $E4^*$ are well accounted for. The electrical activity of $V_3O(C_{2v})$ arises from a_1 and b_1 deep states [Fig. 6(e)]. These are symmetric and antisymmetric dangling-bond states localized at the rightmost and leftmost Si radicals shown in Fig. 6(c). The calculated level positions for $V_3(C_{2v})$, $V_3(D_3)$, and $V_3O(C_{2v})$ are summarized in Table I together with assignments to the experimental data.

V. CONCLUDING REMARKS

We present an experimental observation of a center from a family of mysterious “fourfold coordinated defects” in semiconductor crystals which was predicted by *ab initio* calculations.¹⁻³ Our results confirm the prediction of Makhov and Lewis,³ who showed that the fourfold coordinated configuration could be the lowest-energy state for the neutral V_3 defect in Si. According to the same authors, the small fourfold vacancy clusters in Si would not have energy levels in the band gap and, as a result, they would be electrically and optically inactive, making their direct observation difficult. However, it is found in the present work that the fourfold coordinated V_3 in Si has a shallow acceptor level close to the conduction-band edge. By studying the electron emission from this level, its exact position and symmetry of the FFC V_3 defect have been determined. We also demonstrate that V_3 interacts efficiently with oxygen atoms in O-rich silicon crystals to result in a V_3O defect. V_3O is only stable in the (110) planar C_{2v} symmetric configuration. Like the planar V_3 center, the V_3O complex gives rise to two deep acceptor levels in the upper half of the gap.

It was also predicted by Makhov and Lewis³ that the fourfold coordinated configurations could be the ground states for the V_4 and V_5 defects. Our preliminary DLTS results on epi-Si p^+-n diodes irradiated at room temperature with alpha

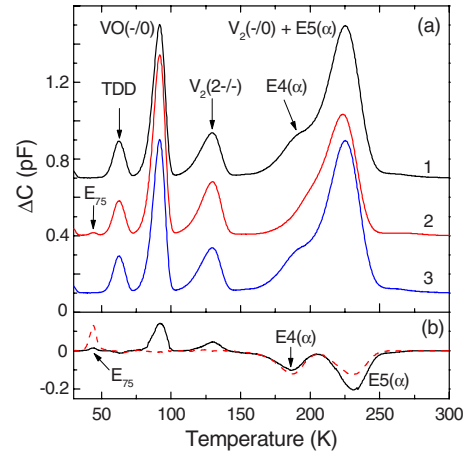


FIG. 7. (Color online) (a) DLTS spectra for an epi-Si p^+-n diode which was subjected to the following subsequent treatments: (1) irradiation with alpha particles from a ^{210}Po source, (2) annealing at 125 °C for 30 min, and (3) forward bias injection with a current density 10 A/cm² for 10 min at 300 K. Measurement settings were $e_n = 80$ s⁻¹, bias -10 V \rightarrow -2 V, and pulse length 1 ms. The spectra are shifted on the vertical axis for clarity. (b) Difference between the DLTS spectra 2 and 3 in (a). For a comparison, the dashed line presents the difference between the DLTS spectra 2 and 1 shown in Fig. 1(a) for an electron-irradiated p^+-n diode.

particles from a ^{210}Po source support this prediction. The DLTS measurements on the diodes irradiated with alpha particles show that the E4 and E5 signals in these diodes consist of contributions from other traps in addition to those related to V_3 (Fig. 7). Similar to the V_3 -related E4 and E5, the alpha-irradiation-induced traps, $E4(\alpha)$ and $E5(\alpha)$, anneal out in the temperature range of 50–150 °C and can be restored by forward current injection in the p^+-n diodes. However, no other traps apart from E_{75} have been detected in the DLTS spectra after the disappearance of the alpha-irradiation-induced E4-E5 traps. We suggest that the E4 and E5 DLTS signals in Si samples irradiated with alpha particles and fast neutrons²⁶ consist of contributions from the V_4 and V_5 defects in addition to those due the V_3 center. Similar to V_3 , the V_4 and V_5 clusters are bistable in the neutral charge state with the FFC configurations being the lowest in energy. The bistabilities of V_4 and V_5 are the origin of annealing- and injection-induced phenomena related to the alpha- and neutron-irradiation-induced E4-E5 traps.²⁶ It appears that in contrast to V_3 , the V_4 and V_5 centers do not have energy levels in the fourfold coordinated configurations.

ACKNOWLEDGMENTS

We would like to thank EPSRC-GB and the Norwegian Research Council for financial support.

- ¹S. Goedecker, T. Deutsch, and L. Billard, Phys. Rev. Lett. **88**, 235501 (2002).
- ²M. D. Moreira, R. H. Miwa, and P. Venezuela, Phys. Rev. B **70**, 115215 (2004).
- ³D. V. Makhov and L. J. Lewis, Phys. Rev. Lett. **92**, 255504 (2004).
- ⁴J. L. Hastings, S. K. Estreicher, and P. A. Fedders, Phys. Rev. B **56**, 10215 (1997).
- ⁵T. E. M. Staab, A. Sieck, M. Haugk, M. J. Puska, T. Frauenheim, and H. S. Leipner, Phys. Rev. B **65**, 115210 (2002).
- ⁶D. A. Abdulmalik and P. G. Coleman, Phys. Rev. Lett. **100**, 095503 (2008).
- ⁷G. D. Watkins and J. W. Corbett, Phys. Rev. **138**, A543 (1965).
- ⁸A. O. Evwaraye and E. Sun, J. Appl. Phys. **47**, 3776 (1976).
- ⁹M. Mikelsen, E. V. Monakhov, G. Alfieri, B. S. Avset, and B. G. Svensson, Phys. Rev. B **72**, 195207 (2005).
- ¹⁰V. P. Markevich, A. R. Peaker, S. B. Lastovskii, L. I. Murin, and J. L. Lindström, J. Phys.: Condens. Matter **15**, S2779 (2003).
- ¹¹R. R. Wixom and A. F. Wright, Phys. Rev. B **74**, 205208 (2006).
- ¹²Y.-H. Lee and J. W. Corbett, Phys. Rev. B **9**, 4351 (1974).
- ¹³V. P. Markevich, A. R. Peaker, S. B. Lastovskii, L. I. Murin, J. Coutinho, A. V. Markevich, V. J. B. Torres, P. R. Briddon, L. Dobaczewski, E. V. Monakhov, and B. G. Svensson, Physica B **404**, 4565 (2009).
- ¹⁴L. Dobaczewski, A. R. Peaker, and K. Bonde Nielsen, J. Appl. Phys. **96**, 4689 (2004).
- ¹⁵P. R. Briddon and R. Jones, Phys. Status Solidi B **217**, 131 (2000).
- ¹⁶J. P. Perdew and Y. Wang, Phys. Rev. B **45**, 13244 (1992).
- ¹⁷J. Coutinho, S. Öberg, V. J. B. Torres, M. Barroso, R. Jones, and P. R. Briddon, Phys. Rev. B **73**, 235213 (2006).
- ¹⁸S. Ögüt and J. R. Chelikowsky, Phys. Rev. Lett. **83**, 3852 (1999).
- ¹⁹J. Coutinho, V. J. B. Torres, R. Jones, and P. R. Briddon, Phys. Rev. B **67**, 035205 (2003).
- ²⁰L. C. Kimerling and J. L. Benton, Appl. Phys. Lett. **39**, 410 (1981).
- ²¹G. D. Watkins and J. W. Corbett, Phys. Rev. **121**, 1001 (1961).
- ²²M. Ahmed, S. J. Watts, J. Matheson, and A. Holmes-Siedle, Nucl. Instrum. Methods Phys. Res. A **457**, 588 (2001).
- ²³M. Moll, E. Fretwurst, M. Kuhnke, and G. Lindström, Nucl. Instrum. Methods Phys. Res. B **186**, 100 (2002).
- ²⁴J. H. Bleka, E. V. Monakhov, B. G. Svensson, and B. S. Avset, Phys. Rev. B **76**, 233204 (2007).
- ²⁵J. H. Bleka, L. Murin, E. V. Monakhov, B. S. Avset, and B. G. Svensson, Appl. Phys. Lett. **92**, 132102 (2008).
- ²⁶R. M. Fleming, C. H. Seager, D. V. Lang, E. Bielejec, and J. M. Campbell, Appl. Phys. Lett. **90**, 172105 (2007); J. Appl. Phys. **104**, 083702 (2008).
- ²⁷G. D. Watkins and J. W. Corbett, Phys. Rev. **134**, A1359 (1964).
- ²⁸A. A. Kaplyanskii, Opt. Spectrosc. **16**, 329 (1964).
- ²⁹J. W. Corbett, J. C. Bourgoin, L. J. Cheng, J. C. Corelli, Y.-H. Lee, P. M. Mooney, and C. Weigel, in *Radiation Effects in Semiconductors*, edited by N. B. Urli and J. W. Corbett, Institute of Physics Conference Series No. 31 (Institute of Physics, London, 1976), p. 1.
- ³⁰M. Mikelsen, E. V. Monakhov, B. S. Avset, and B. G. Svensson, Phys. Scr. **T126**, 81 (2006).
- ³¹L. I. Murin, B. G. Svensson, J. L. Lindström, V. P. Markevich, and C. A. Londos, Solid State Phenom. **156-158**, 129 (2010).